https://doi.org/10.22320/s0718221x/2026.12
ARTÍCULO

Influence of particle size and blending ratio on the physical and mechanical properties of falcata sawdust–recycled LDPE wood–plastic composites

Juanito P. Jimenez, Jr.[1] https://orcid.org/0000-0001-7389-1826

[1]Department of Science and Technology, Forest Products Research and Development Institute College. Laguna, Philippines.

Corresponding author: juanito.jimenez@fprdi.dost.gov.ph

Abstract:
The increasing accumulation of wood and plastic waste necessitates the development of sustainable, value-added materials such as wood-plastic composites (WPCs). This study investigated the feasibility of utilizing *Falcataria moluccana* (falcata) sawdust as a reinforcing filler in a recycled low-density polyethylene (LDPE) matrix. WPCs were fabricated via twin-screw extrusion using three sawdust particle sizes—P20R40 (0,840 - 0,400 mm), P40R60 (0,400 - 0,250 mm), and P60 (<0,250 mm)—at blending ratios of 30:70 and 40:60 (sawdust:LDPE, by weight). Physical properties, including relative density, moisture content, water absorption, and thickness swelling, were evaluated alongside mechanical performance according to ASTM standards. The results demonstrated that the incorporation of sawdust produced WPCs with physical stability and hygroscopic properties comparable to or superior to those of the pure recycled LDPE control. Mechanical analysis revealed a significant reinforcement effect; the inclusion of sawdust enhanced both the tensile and flexural strength and modulus of the composites. Specifically, finer sawdust particles (<0,250 mm) and a 30:70 sawdust-to-LDPE ratio yielded the optimal overall mechanical performance. However, impact strength tests indicated that the wood filler increased material brittleness, as the neat LDPE significantly outperformed all WPC treatments in energy absorption. Overall, this study concludes that falcata sawdust is a viable natural fiber for reinforcing recycled LDPE, offering a sustainable pathway for upcycling waste into rigid composite materials, provided that applications account for the inherent reduction in impact resistance.

Keywords: Falcataria moluccana, low-density polyethylene (LDPE), mechanical properties, particle size, recycled plastics, wood plastic composites (WPC).

Received: 24.08.2024
Accepted: 30.03.2026

Introduction

Wood-plastic composites (WPC/WPCs) blend wood particles and thermoplastic materials from post-consumer recycled plastics and sawdust generated by lumber mills and furniture factories (Clemons 2002, Caulfield *et al.* 2005). Produced for several decades now in various countries, they have emerged as a compelling eco-friendly substitute for conventional materials across diverse industries owing to their multifaceted properties including durability, adaptability, and sustainability. Worldwide, WPCs find extensive use as outdoor deck floors, as well as railings, fences, landscaping timbers, cladding, siding, park benches, molding, trim, window and door frames, and indoor furniture (Smith and Wolcott 2006, Spear *et al*. 2015, Xu *et al*. 2021).

Since the 1980s, the success of WPCs has been evident across a spectrum of industries spanning construction, automotive, furniture, electronics, and beyond. In the Philippines, there is a growing exploration of various plastics, whether virgin or recycled, with notable leaning towards the utilization of recycled waste plastics sourced from Material Recovery Facilities (MRFs) and combined with agricultural processing wastes (Paglicawan *et al*. 2025) from industrial processes and wood-based industries such as sawmills, veneers, plywood, and furniture manufacturing (Jimenez *et al*. 2013, Paglicawan *et al*. 2022). This surge in interest can be attributed, in part, to the influx of imported WPCs into the country, which has sparked a realization of the untapped potential of locally available natural fibers.

Driven by an increasing market demand for WPCs, plastic manufacturers are actively seeking opportunities to capitalize on all viable natural fibers sourced from agricultural and forest industries. While technically all natural fibers can serve as fillers for thermoplastics, their suitability varies due to differences in chemical composition. Studies have revealed that natural fibers, whether derived from forest tree species or agricultural plants, must be carefully evaluated for compatibility with plastics to enable their conversion into diverse WPC products

(Berger and Stark 1997, Caulfield *et al*. 2005, Gacitúa and Wolcott 2009, Berzin and Vergnes 2021, Xu *et al*. 2021).

Studies on the physical and mechanical properties of WPCs have been a cornerstone of their development, particularly when introducing new natural fibers from wood processing wastes or agricultural and industrial byproducts. A review of existing literature reveals several key findings. In exploring the effect of different plastic matrices on physical properties, Najafi *et al.* (2008) found that WPCs made with polypropylene (PP) exhibit higher water absorption than those with polyethylene (PE), and that composites from recycled plastics absorb more water than those from virgin materials. The kinetics of water absorption have also been shown to follow a Fickian diffusion process (Tajvidi *et al.* 2006, Najafi *et al*. 2008), with significant variations observed between different fiber types. Furthermore, water uptake of WPCs increases with the increase in fiber content (Chaharmahali *et al.* 2010) as well as with larger particle sizes (Khonsari *et al.* 2015). Research on mechanical properties has shown that WPCs from recycled plastics can possess similar strength and stiffness as those made from virgin plastics (Najafi *et al.* 2006). However, the proportion and compatibility of wood flour and polymer are critical factors, as an increase in fiber content beyond an optimal level can lead to reduced flexural strength and impact resistance due to lack of compatibility between phases (Chaharmahali *et al*. 2008).

Despite these advancements, a significant knowledge gap remains regarding the specific interfacial compatibility and reinforcing potential of low-density tropical wood species when combined with recycled low-density polyethylene (LDPE). While high-density polyethylene (HDPE) and PP are extensively documented in WPC literature, there is a lack of empirical data on how the unique anatomical and chemical characteristics of fast-growing plantation species, such as falcata, interact with the more flexible LDPE matrix, particularly in non-compatibilized

systems. This lack of specific performance data hinders the industrial adoption of these specific waste streams for structural or semi-structural applications.

One of the identified concerns highlighted in the Philippine Council for Agriculture, Aquatic, and Natural Resources Research and Development's (PCAARRD) Industry Strategic Plan for Industrial Tree Plantation Species (ITPS) is the large volume of unutilized plantation wastes, including sawdust, log trims, veneer round-outs, veneer log cores, and barks generated from the processing of falcata (*Falcataria moluccana* (Miq.) Barneby & J.W. Grimes), yemane (*Gmelina arborea* Roxb.) and other ITPS (Israel and Bunao 2017, Jimenez *et al*. 2021). These processing wastes primarily end up as fuel for boilers, contributing to increased greenhouse gas emissions. Converting these wastes into WPCs offers a promising alternative for resource recovery.

Among the post-consumer thermoplastic wastes, LDPE plastic constitutes a significant volume generated daily in urban cities contributing heavily to environmental pollution (World Bank Group 2021). Recycling these plastics into valuable products like WPCs presents a viable solution to the environmental challenges associated with plastic waste accumulation. Known for its flexibility, toughness, and ease of processing, LDPE can potentially serve as a matrix material in WPCs (Posch 2011, Ramli 2024). However, research on this area has been limited, particularly regarding its blending compatibility and properties with ITPS such as falcata.

This study investigated the compatibility between recycled LDPE and sawdust obtained from sawmilling of falcata logs. Falcata was selected due to its high production volume in the Philippines (Jimenez *et al.* 2015, Alipon *et al.* 2021, Jimenez *et al.* 2022, FMB-DENR 2023). By addressing the aforementioned knowledge gap, this research aimed to evaluate the physical and mechanical properties of the resulting composite by varying the wood-sawdust ratio and particle size. It was hypothesized that incorporating falcata would enhance the mechanical

properties of LDPE in WPCs, contributing to resource conservation and circular economy initiatives.

Materials and methods

Experimental materials

Seven-year-old falcata trees were sourced from Bayugan, Agusan del Sur, Mindanao, Philippines. According to a technical information leaflet (n.d.) published by the Forest Products Research and Development Institute (FPRDI), the basic chemical composition of falcata wood is as follows: holocellulose content, 71,70 %; alpha-cellulose, 53,50 %; lignin, 24,70 %; pentosans, 16,35 %; alcohol-benzene extractives, 2,10 %; hot water solubility, 1,25 %; 1 % NaOH solubility 14,60 %; and ash content, 0,40 %.

The falcata logs were sawn into lumber using the FPRDI's Wood-Mizer. The sawdust generated was collected and oven-dried at 103 ºC ± 2 ºC for 8 h with mixing every 2 h to ensure uniform drying. After drying, the sawdust was cooled and mechanically sieved through various mesh sizes (20 mesh, 40 mesh and 60 mesh). The initial sieving of the four sacks of sawdust was conducted for 5 min, 10 min, and 15 min to determine the optimal sieving time required to screen 100 g of sawdust. Four sieving trials were performed for each duration to assess the practicality of longer sieving periods. The sieving yield for each duration and mesh size was calculated and compared. Free-settled bulk density of sieved falcata sawdust was determined.

The recycled LDPE pellets used in the experiment were purchased from Reinheart Marketing, Inc., a plastic recycling plant in Valenzuela City, Philippines. The bulk density of the LDPE was also determined. Differential Scanning Calorimetry (DSC) confirmed that the recycled pellets were composed of 88,2 % LDPE and 11,8 % ethylene vinyl acetate (EVA) copolymer. The obtained melt flow rate (MFR) of the recycled LDPE used in this study was 4,32 g/10 min (measured at 190 °C and 2,16 kg load).

Compounding experiment

The compounding ratios of falcata sawdust to LDPE is shown in Table 1. For each combination, i.e. mesh-SD:LDPE, 750 g of mixture was made.

Table 1: Matrix of compounding of SD:LDPE at various mesh sizes

Ratio SD:LDPE	Mesh Code	Sawdust Size (mm)
30:70	P20R40	0,841 - 0,400
30:70	P40R60	0,400 - 0,250
30:70	P60	< 0,250
40:60	P20R40	0,841 - 0,400
40:60	P40R60	0,400 - 0,250
40:60	P60	< 0,250

The 40:60 combination of P20R40 clogged the exit nozzles of the WPC strands, hence it was discontinued.

The mixture of falcata sawdust and recycled LDPE was melt compounded in a counter-rotating twin-screw extruder (Scientific LabTech Eng'g Company Ltd) with an L/D ratio of 40:1 to produce WPC strands (Figure 1). The continuously extruded strand was transformed into pellets using a pelletizer. The temperature profiles used during the process were as follows: Zone 1 = 180 °C, Zone 2 = 180 °C, Zone 3 = 180 °C, Zone 4 = 190 °C, Zone 5 = 190 °C, Zone 6 = 190 °C, Zone 7 = 170 °C, Zone 8 = 170 °C, Zone 9 = 160 °C and Zone 10 = 160 °C.

Additional parameters included a hopper speed of 11,5 rpm (1,20 rad·s^{-1}), screw rotation of 200 rpm (20,94 rad·s^{-1}), and pelletizer speed of 9,7 rpm (1,02 rad·s^{-1}).

It should be noted that no coupling agents were incorporated into these compounding experiments to allow the establishment of baseline data for the material properties without such additives. Further, the inherent presence of polar Ethylene-Vinyl Acetate (EVA) copolymer within the recycled LDPE matrix was hypothesized to enhance the interfacial bonding between the wood particles and the plastic matrix. This is because EVA, being a polar molecule, can facilitate hydrogen bonding with the hydroxyl groups (OH) of wood, thereby improving compatibility (Faker *et al*. 2008, Aumnate *et al.* 2010, Zimmermann *et al*. 2014, Hu *et al*. 2020) The compounded WPC at the 40:60 SD:LDPE of P20R40 mesh lumped and blocked the exit nozzles of the WPC strand due to larger particle size and higher percentage mass compared with 30:70 SD:LDPE of P20R40 mesh. Hence, compounding of the sawdust and LDPE at P20R40 mesh of 40:60 combination was discontinued.

Production and testing of experimental boards

The composite pellets were oven-dried to below 3 % moisture at 80 °C for 2 h in a vacuum oven. A mass of 150 g of WPC pellets was then placed in a square mold (0,3 cm × 20 cm × 20 cm) enclosed between aluminum sheets. The mold was heated to 180 °C in a compression molding machine and pressed at 50 kg·cm^{-2} for 5 min. Entrapped air was relieved by applying step-down pressure prior to removing the samples from the hot press. The boards were subsequently transferred to a cold press for 5 min, then conditioned for one week at 23 ± 2 °C and approximately 65 % relative humidity (RH).

After conditioning, the boards were cut using a portable jigsaw to the required dimensions for physical and mechanical testing, in accordance with the specifications of the relevant ASTM standards.

Physical properties testing

Five samples from each treatment combination (as shown in Table 1) were tested for physical properties following ASTM D1037-99 (2017) and ASTM D2395-17 (2022). A modified sample size of 0,3 cm × 2 cm × 6 cm was used for determining moisture content (*MC*), relative density (*RD*), water absorption (*WA*), and thickness swelling (*TS*).

Initial weight (*Wi*) was measured using a Shimadzu analytical balance with a precision of 0,0001 g. Initial thickness (*Ti*) was recorded at three equidistant points across the width using a Mitutoyo digital thickness gauge with a precision of 0,001 mm.

Due to slight thickness variations, volume (*Vw*) was determined using the water immersion method based on Archimedes' principle. The setup consisted of a Boeco digital top-loading balance (precision: 0,001 g), a 500-mL beaker filled with distilled water, and a wooden stick with a fine needle affixed to the tip. The stick was clamped vertically to a metal rod stand, allowing the sample to be mounted on the needle tip. The balance was tared to zero with the water-filled beaker in place. Each sample was carefully submerged until fully immersed, ensuring no contact with the beaker walls or bottom. The balance reading during submersion represented the weight of the displaced water, which corresponded to the sample's *Vw*. Samples were then oven-dried at 103 °C until a constant weight (*Wo*) was reached.

MC was calculated using the Equation 1:

$$MC\ (\%) = \frac{(W_i - W_0)}{W_0} 100 \quad (1)$$

RD was computed as:

$$RD = \frac{W_0}{V_w}$$

Oven-dry thickness (*To*) was measured at three points, and the values of *Wo* and *To* were used as reference for *WA* and *TS* calculations after 2 h and 24 h of water immersion with Wf as the final weight and Tf as the final thickness.

WA was determined using the Equation 2:

$$WA\ (\%) = \frac{(W_f - W_0)}{W_0} 100 \quad (2)$$

TS was computed as Equation 3:

$$\text{TS}\ (\%) = \frac{(T_f - T_0)}{T_0} 100 \quad (3)$$

Mechanical properties testing

Five samples per treatment combination were also tested for mechanical properties. All test specimens were conditioned at 23 °C and 50 % RH for one week prior to testing.

Tensile strength was determined using a Shimadzu Autograph AGS-X Universal Testing Machine equipped with a 10 kN load cell, following ASTM D638-02 (2017). Type I dumbbell-shaped specimens were tested at a crosshead speed of 5 mm·min^{-1} and a gauge length of 50 mm.

Flexural tests were conducted based on ASTM D790-15e2 (2017) and ASTM D7031-11 (2019) using specimens with dimensions of 127 mm × 12,7 mm × 3 mm, under a three-point bending configuration. The support span was set at 48 mm, with a crosshead speed of 1,28 mm·min^{-1} and a 10 kN load cell.

Impact strength was evaluated using the Izod method, in accordance with ASTM D256-10e1 (2018), using a Zwick/Roell 5,5 P pendulum impact tester. Unnotched specimens with dimensions of 63,5 mm × 12,7 mm × 3 mm were used.

A schematic diagram of the process-from production of composite pellets, molding via compression, to physical (*RD, MC, WA,* and *TS*) and mechanical (tensile, flexural, impact strength) testing-is presented in Figure 1.

Microscopic observations of the WPC samples

Microscopic observations of the WPC samples were performed using a Keyence VHX-7000 digital microscope. The morphology and surface characteristics of the compounded WPC pellets and boards were examined. These were compared against the recycled LDPE reference material.

Statistical analysis

The physical and mechanical properties tested were analyzed using a Completely Randomized Design (CRD) in a one-way ANOVA. In this model, the treatments were defined as the unique combinations of two experimental factors: sawdust particle size (P20R40, P40R60, and P60) and sawdust-to-LDPE blending ratio (30:70 and 40:60). Treatment means were separated using Duncan Multiple Range Tests (DMRT) at a significant level of $p < 0,05$. Statistical analysis was carried out using SAS 9,4 for Windows.

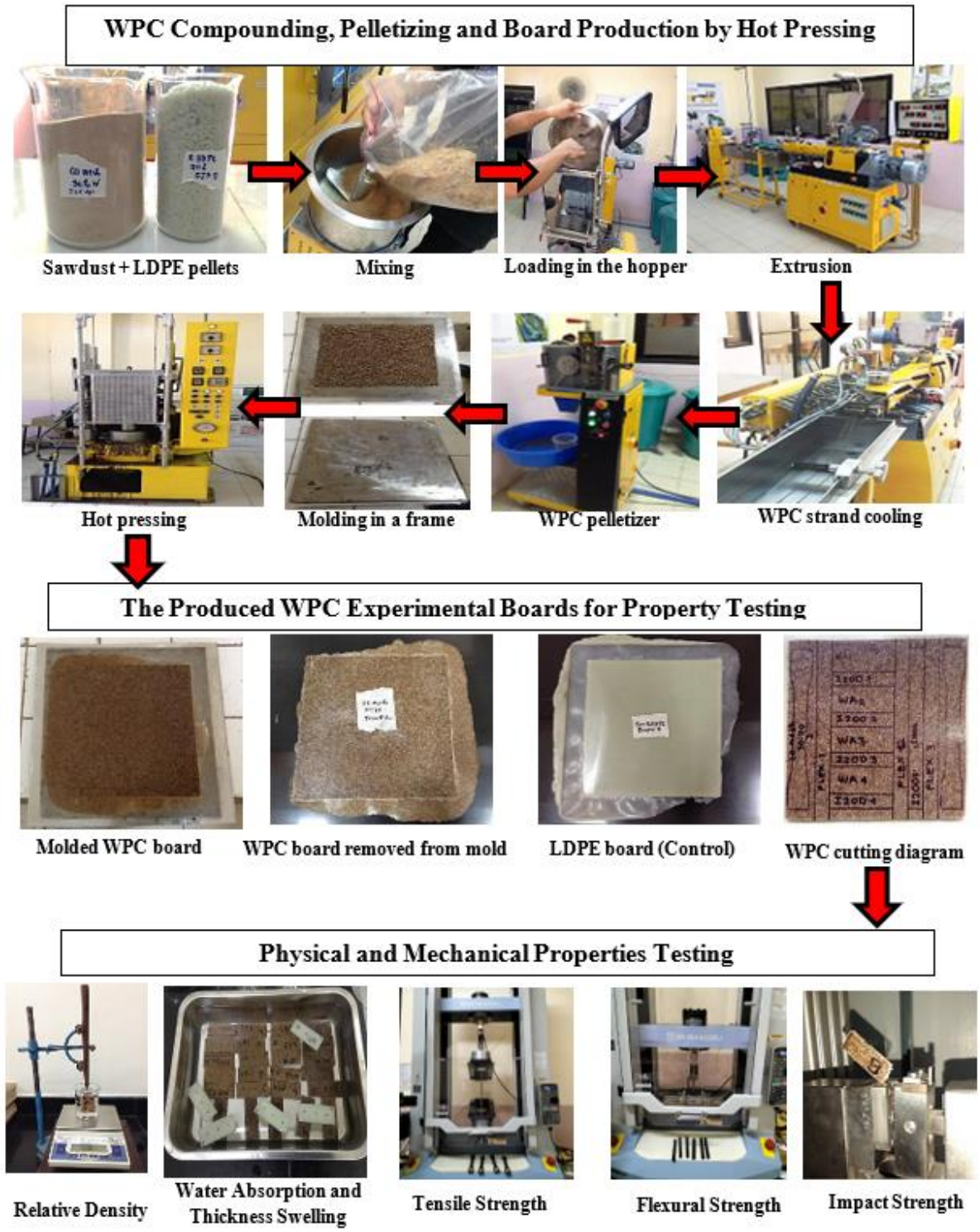

Figure 1: Schematic illustrations of the production process for compounded WPC pellets, followed by the manufacturing of experimental boards through compression molding, and the subsequent physical and mechanical property testing.

Results and discussion

Sieving property of falcata sawdust

Falcata sawdust sieved for 5 min, 10 min, and 15 min produced different retention proportions across mesh sizes (Table 2). At 5 min and 10 min of sieving, the highest retention occurred in the R20 fraction (>0,841 mm). However, at 15 min, the highest retention shifted to the P20R40 fraction (0,841 - 0,400 mm). For every 100 g of sawdust sieved, approximately one-third remained in R20, another third in P20R40, and the remaining third was distributed between P40R60 (0,400 mm - 0,250 mm) and P60 (<0, 250 mm). Since the present study used only sawdust passing through 20 mesh, 40 mesh, and 60 mesh sizes, roughly 33 % of the sieved material in the R20 fraction was excluded from WPC production but could still be utilized for other value-added applications such as sawdust briquettes for solid fuel (Eduagin *et al.* 2021) or as a precursor for activated carbon production (Granada *et al.* 2024).

Table 2 shows that with every 5 min increase in sieving time, the yield of the R20 fraction decreased, with the reduction redistributed across finer mesh fractions. However, the incremental gain in finer fractions was small. For example, the P60 fraction increased only from 12,56 g at 5 min to 13,20 g at 10 min, and 15,17 g at 15 min. Given the minimal increase in fine-particle yield relative to the additional time and energy cost, extending sieving beyond 5 min is impractical. Thus, a sieving time of 5 min was deemed sufficient for this study.

The particle size distribution of sawdust is influenced not only by the physical and anatomical properties of the wood source but also by the sawing process itself (Maharani *et al*. 2010). Intrinsic factors such as density, grain orientation, moisture content, and extractive composition interact with tool-related characteristics including blade type, sharpness, and tooth geometry

and operational parameters such as feed rate, cutting speed, and whether a band saw or circular saw is used (Mračková *et al.* 2016, Bello 2017). These variables collectively determine the amount of material retained in each mesh category during sieving. Previous studies on the sieve analysis of wood sawdust are not directly comparable with the present work because they employed substantially different mesh size ranges. For example, Bello (2017) used #8 mesh to #40 mesh screens, which are suited for coarser particles, while Vítěz and Trávníček (2010) categorized particles into 6 mm, 0,1 mm, and <0,1 mm size classes ranges that differ markedly from the finer particle fractions examined in the present study.

In the context of WPC manufacturing, particle size, geometry, and surface area significantly influence polymer encapsulation, interfacial adhesion, and final mechanical performance (Stark and Rowlands 2003, Gacitúa and Wolcott 2009, Gozdecki and Wilczyński 2015, Khonsari *et al*. 2015, Rahman *et al*. 2018). Coarser particles, such as those in the P20R40 mesh fraction, were observed to cause blockage of the extruder strand exit nozzles during WPC compounding at a loading level of 40 wt.% falcata sawdust. Finer particles generally provide better dispersion and bonding within the polymer matrix due to their larger specific surface area. However, an excessive proportion of fines may lead to processing difficulties due to particle agglomeration and reduced mechanical strength attributed to poor load transfer (Delviawan *et al.* 2019, Sandquist *et al.* 2020). Considering these trade-offs, the present study used only material passing through the 20-mesh screen, further classified into four mesh categories (Table 2), to achieve an optimal balance between particle size uniformity and processing efficiency.

MC showed a decreasing trend as sawdust particle size decreased, although variations in mixing thoroughness during drying could also have influenced the results. In accordance with established practice, the sawdust used in this study was conditioned to a *MC* not exceeding 3 %, a threshold also applied in comparable WPC systems (Kamdem *et al.* 2004, Paglicawan *et*

al. 2022). The free-settled bulk density of falcata sawdust increased with mesh number, consistent with Zepeda-Cepeda *et al.* (2021) findings on particle density trends in sawdust. This relationship is expected because as mesh number increases, particle size decreases, allowing finer particles to pack more efficiently and achieve greater compaction even under free-settling conditions.

Table 2: Sieved yield, moisture content and bulk density of falcata sawdust

Mesh Code (Size, mm)	Average Yield of Sawdust per 100 g sieving*			Moisture Content, %	Bulk Density, kg/m³
	5 min	10 min	15 min		
R20 (>0,841)	33,74	32,46	28,91	2,12 (*0,02*)	88
P20R40 (0,841 - 0,400)	31,06	31,79	31,48	1,99 (*0,03*)	96
P40R60 (0,400 - 0,250)	22,65	22,55	24,44	1,96 (*0,03*)	103
P60 (<0,250)	12,56	13,20	15,17	1,85 (*0,03*)	112
Total	100	100	100	-	-

* Average of 4 sieving trials;
() Italicized values in parentheses are standard deviations of the means for Moisture Content.

Physical properties of WPC

Microscopic observations of the WPC pellets and boards

Microscopic imaging of LDPE pellets and WPC pellets containing falcata sawdust of varying particle sizes and loadings revealed distinct morphological differences (Figure 2a and Figure 2b). LDPE pellets exhibited a greenish-gray color with microvoids (Figure 3 and Figure 4a)

present on the cross-section of the pelletized strands, with diameters ranging from 522-634 μm and depths of about 687 μm (Figure 4a). These voids likely originated from entrapped air or incomplete polymer melt consolidation during extrusion. They might have also resulted from the immiscibility of LDPE and EVA blends, which promoted phase separation, as reported by Aumnate *et al*. (2010) and Faker *et al*. (2008). In contrast, WPC pellets exhibited progressively smoother surface textures with decreasing sawdust particle size (Figure 2a and Figure 2B). Finer particles (P60 mesh) appeared more uniformly dispersed within the matrix, minimizing surface irregularities compared with coarser fractions (P20R40 mesh). This observation aligns with reports that finer wood flour enhances matrix wetting and flow uniformity (Clemons 2010, Zimmermann *et al.* 2014). Although microvoids were still present in WPC pellets, their diameters and depths were smaller than those in control LDPE (Figure 3a, Figure 4a and Figure 4b), likely because the filler particles interfered with void coalescence during cooling. High-resolution imaging of LDPE and WPC boards (20× magnification) confirmed the particle size differences between mesh fractions (Figure 5a, Figure 5b, Figure 5c, Figure 5d, Figure 5e, Figure 5f). The P20R40 mesh at 30 wt.% loading contained the largest visible particles (Figure 5a), whereas P60 mesh exhibited a finer, more homogeneous distribution (Figure 5c). However, at higher loadings (40 wt.%), P40R60 and P60 mesh samples displayed localized particle agglomerations, consistent with particle-particle interactions overcoming polymer wetting forces at elevated filler contents (Ashori *et al*. 2011, Zimmermann *et al.* 2014, Pożoga and Szczepanek 2021). Microscopic characterization of LDPE-falcata sawdust WPC pellets revealed important implications for downstream processing and application. The smoother surfaces and smaller voids observed in pellets with finer sawdust particles imply enhanced melt flow during injection and extrusion molding, which can reduce weld-line weaknesses and improve dimensional stability. This aligns with the finding that increased wood filler content when well-distributed enhances density, stiffness, and surface finish in recycled WPC

formulations (Gomes *et al*. 2023, Samyn 2024). These microstructural improvements correspond with the mechanical performance observed in this study, demonstrating the potential suitability of LDPE–falcata WPCs for value-added applications in construction and consumer products.

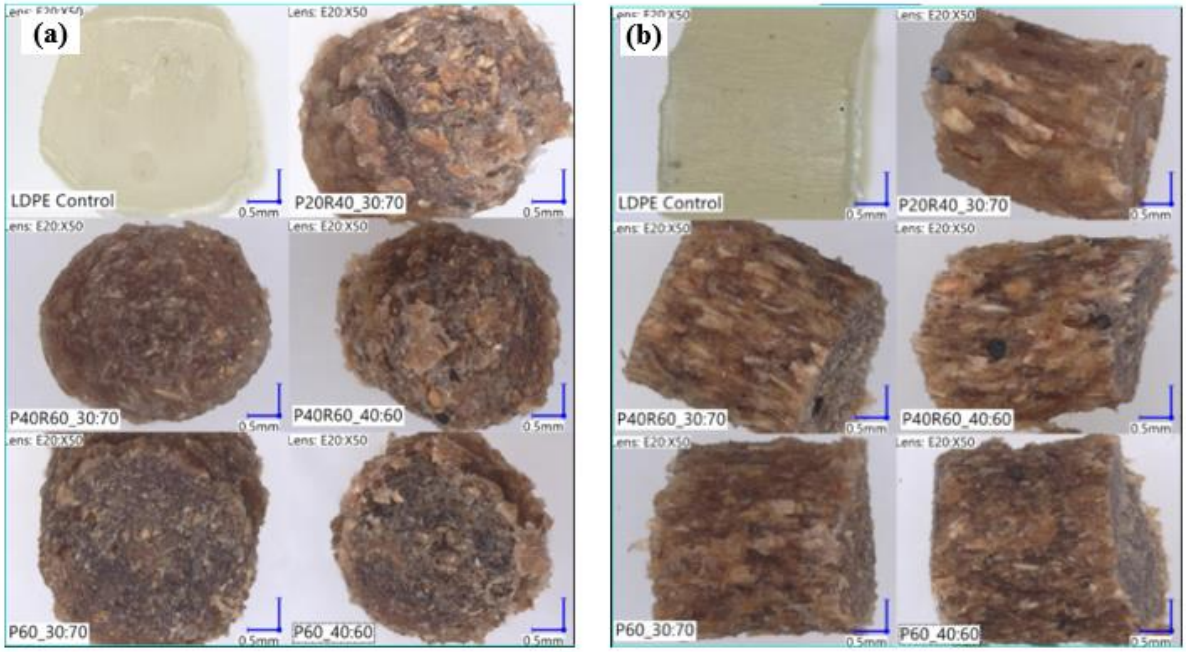

Figure 2: Microscopic images of LDPE and WPC pellets: (a) cross-sectional and (b) side-sectional views. The WPC pellets exhibit progressively smoother surface textures as the sawdust particle size decreases.

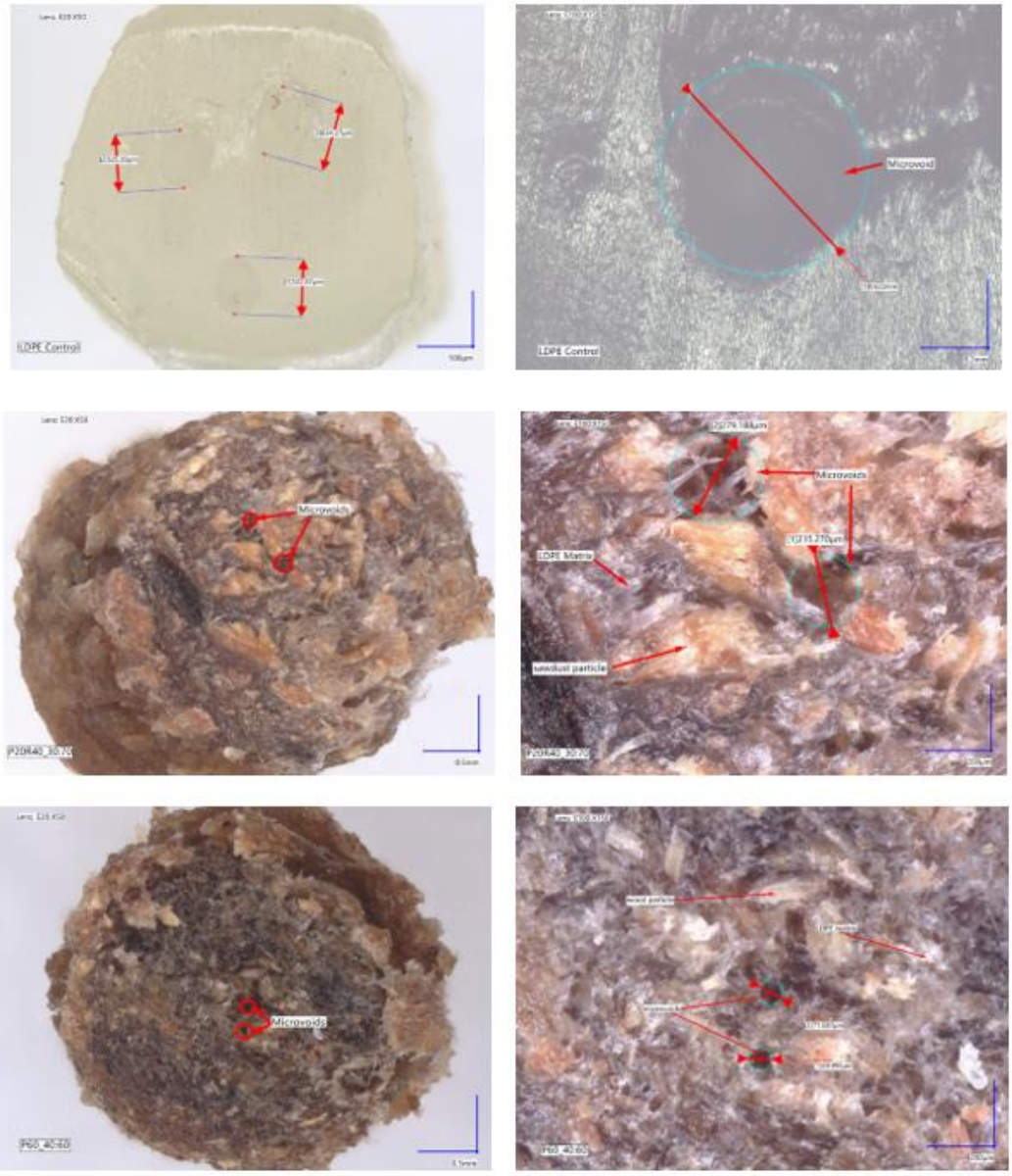

Figure 3: Cross-sectional microscopy of LDPE and WPC pellets showing the effect of sawdust mesh size on microvoid formation. The LDPE pellets contain three large microvoids (522-634 µm), while the P20R40-30:70 WPC pellets show medium-sized microvoids (215-279 µm), and the P60-40:60 WPC pellets exhibit the smallest microvoids (69-72 µm).

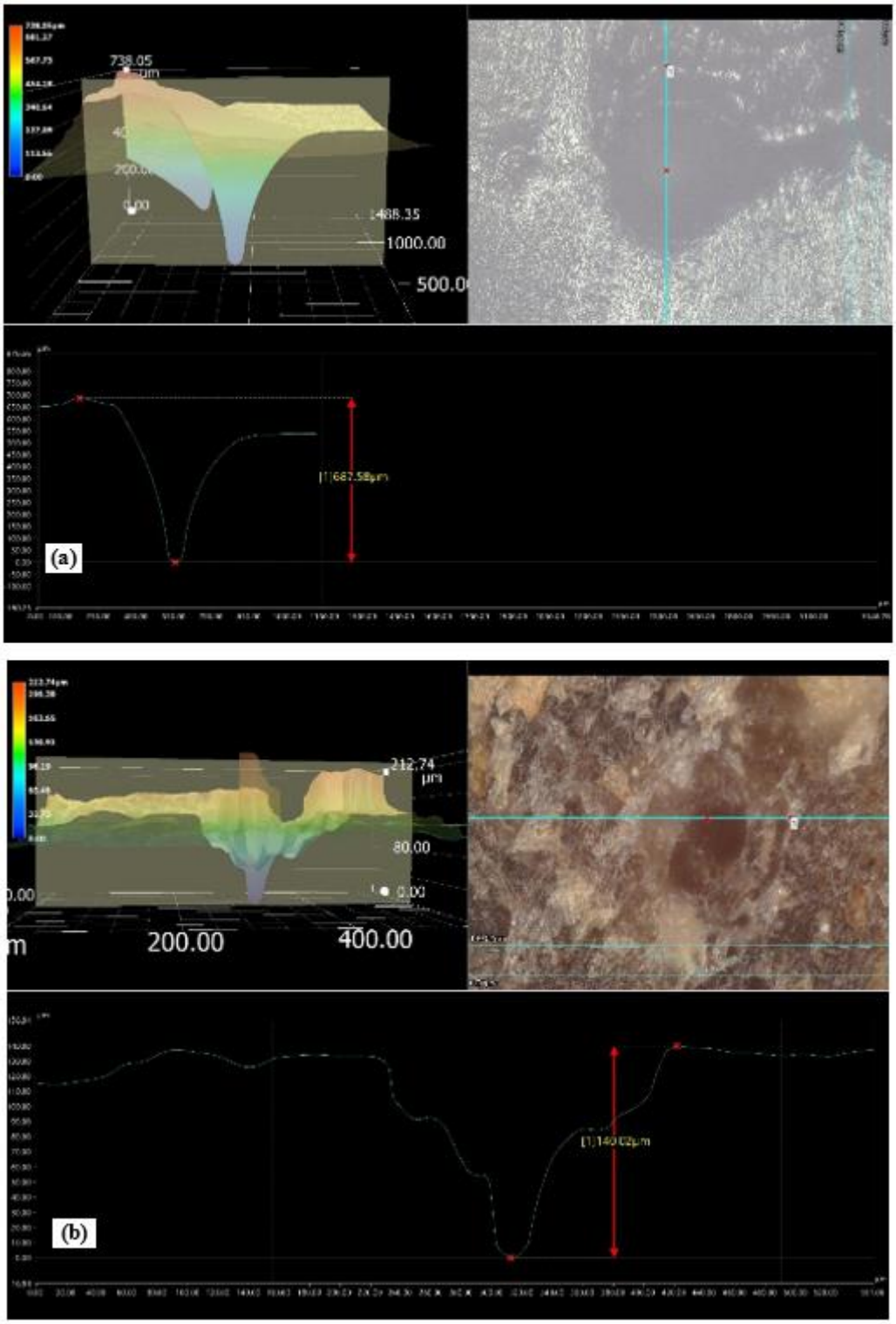

Figure 4: Microscopic analysis of microvoids in LDPE and WPC pellets: (a) a micrograph showing the measured depth of a microvoid in an LDPE pellet, recorded at 687,58 µm and (b) a micrograph showing a significantly smaller microvoid in a compounded WPC pellet, with a measured depth of 140,02 µm. The images illustrate how the addition of wood flour reduces the size of microvoids.

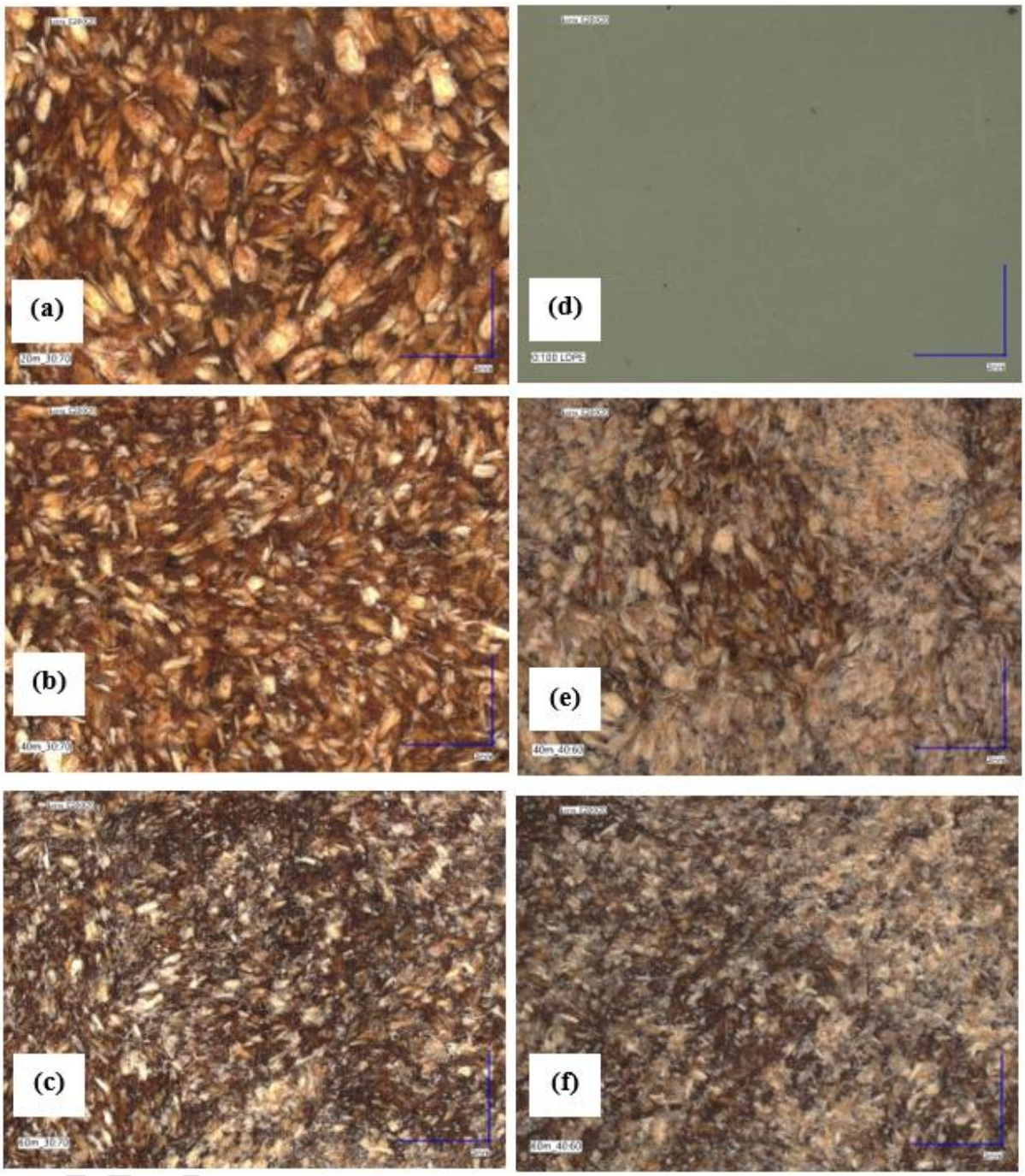

Figure 5: Images of WPC boards made from falcata sawdust and recycled low-density polyethylene (LDPE): (a-c) WPC boards with a 30:70 sawdust-to-LDPE ratio using particle mesh sizes of (a) P20R40, (b) P40R60, and (c) P60; (d) control board made from LDPE; (e-f) WPC boards with a higher 40:60 sawdust-to-LDPE ratio, using particle mesh sizes of (e) P40R60 and (f) P60. Boards with a higher sawdust percentage show evidence of particle agglomeration in certain areas.

Moisture content and relative density

The *MC* of the conditioned boards showed a statistically significant variation ($p<0,0001$) across the sample groups (Table 3). The LDPE control (0:100), exhibiting zero percent MC, significantly differed from all WPC combinations, which ranged from 0,80 % to 1,30 %. This result is attributed to the introduction of sawdust as a hydrophilic component into the otherwise hydrophobic LDPE matrix, making the composite slightly hygroscopic due to the inherent water-absorbing nature of wood particles (Clemons 2010).

The results on the influence of the composition indicated that the quantity of wood sawdust is a more critical determinant of *MC* than the particle size. Increasing the sawdust content from 30 wt.% to 40 wt.% significantly increased moisture absorption. Specifically, the P40R60 sample showed a substantial increase in *MC*, from 0,72 % (at 30:70 ratio) to 1,30 % (at 40:60 ratio), while the P60 samples increased from 0,80 % to 1,03 %, This observed trend is explained by the greater total mass of hygroscopic wood particles within the composite at higher loadings, which provides more available hydroxyl groups for hydrogen bonding with atmospheric moisture (Espert *et al.* 2004). This finding is strongly consistent with literature demonstrating that increasing fiber loading significantly elevates the moisture content of WPCs similar to Rahman *et al.* (2013) who reported an increasing *MC* in flat-pressed WPC boards from 0,92 % (40 wt. % of sawdust) to 2,15 % (70 wt. % of sawdust).

Conversely, within the studied sawdust particle size range, a decrease in particle size did not yield a statistically significant effect on the composite's ability to absorb moisture. For example, at the 30:70 ratio, no significant difference in average *MC* was found across varying particle sizes. This suggests that the total number of available hydroxyl groups, which are the primary sites for moisture absorption, is predominantly governed by the total wood mass rather than

the particle size distribution (Chaharmahali *et al.* 2010, Flores-Hernandez *et al.* 2014). Therefore, in applications where moisture resistance is crucial, optimizing the wood-to-polymer ratio is a more effective strategy than adjusting the sawdust particle size.

The *RD* showed significant differences across all sample groups ($p<0,0001$). The LDPE control (0:100) exhibited an *RD* of 0,95, which was significantly lower than the WPC samples, which ranged from 1,02 to 1,09. This disparity was qualitatively confirmed by buoyancy testing. The recycled LDPE control floated in water (*RD*<1,0), whereas all WPC samples sank (*RD*>1,0).

The shift toward a higher RD values in the WPCs is explained by the fundamental density of the wood material itself. While loose sawdust has low bulk density due to entrapped air, the wood's true cell wall density is significantly higher ranging from 1,4 to 1,5 $g.cm^{-3}$ (Kellogg and Wangaard 1969, Sun 2005). During the high-temperature and high-pressure processing of WPCs, the voids within the wood's cellular structure collapse as the polymer matrix melts and infiltrates the particles. This densification process causes the effective density contribution of the wood filler to shift towards its higher intrinsic material density (Clemons 2010), resulting in an overall density greater than 1,0. The present study is consistent with Rahman *et al* (2013), who reported a density of 1,05 $g{\cdot}cm^{-3}$ for the 40:60 ratio of sawdust and recycled PET

The results further indicate that both the amount of filler loading and particle size of sawdust significantly influenced the final RD. Among the WPC samples, the highest *RD* was observed in P60 (at 40:60 ratio), while the lowest was in P20R40 (at 30:70 ratio). The particle size effect is linked to the packing efficiency and void reduction. Finer particles (P60) allow for denser packing and better interfacial wetting resulting in a lower void content compared with the P20R40 particles. However, the processing method also plays a vital role. Extruded WPCs using a high-shear method have been reported to reach significantly higher densities of 1,21 to 1,23 $g{\cdot}cm^{-3}$ (Chaudemanche *et al.* 2018). Furthermore, the moisture content of the wood fibers during compounding contributed to void formation (Bledzki and Gassan 1999). It is plausible

that the smaller particles in P60, dried more thoroughly and packed more efficiently, resulting in less steam generation and subsequent void formation, and consequently, a denser final composite. This understanding is crucial for optimizing falcata sawdust-based WPC formulations to meet specific density requirements for various industrial applications.

Water absorption and thickness swelling

The results for *WA* and *TS* demonstrate a clear trend where WPC samples absorbed significantly more water than the LDPE control. The ANOVA showed a statistically significant difference in mean *WA* for both the 2-h ($p<0,0001$) and 24-h ($p=0,007$) periods, with a similar trend observed for *TS* at both time points ($p<0,0001$ and $p=0,0003$, respectively). This behavior is primarily attributed to the hydrophilic nature of the sawdust filler. The presence of abundant hydroxyl groups in the wood particles facilitates moisture uptake through the formation of hydrogen bonds with water molecules, thereby increasing the overall hygroscopicity of the composite (Bledzki and Gassan 1999, Flores-Hernandez *et al.* 2014, Radoor *et al.* 2021, Antwi-Boasiako *et al.* 2022).

In contrast, the LDPE matrix is inherently hydrophobic and typically exhibits minimal water absorption (Kormin *et al.* 2019). The observed water absorption in the control LDPE is likely a result of two factors: physical entrapment of water within microvoids and a minor degree of chemical interaction due to the polar ethylene vinyl acetate (EVA) component within the recycled LDPE (Aumnate *et al.* 2010, Pham 2021). The presence of these polar groups causes the recycled LDPE to behave differently from a pure LDPE polymer, which partially accounts

for the observed moisture uptake. These factors, supported by the microscopic evidence in Figure 3 and Figure 4, clarify the reasons for the specific water absorption behavior in the LDPE control (0:100).

Within the WPC samples, *WA* and *TS* varied significantly depending on the sawdust particle size and ratio. For both the 2-h and 24-h periods, the highest *WA* and *TS* were consistently observed in the 30:70 WPC with a P20R40 particle size distribution. Conversely, as the sawdust particle size decreased, a significant reduction in both *WA* and *TS* was observed. For instance, the 30:70 WPC with the P60 particle size showed the lowest WA and TS among all WPC samples for the 24-h period.

These finding are directly explained by the size of the wood particles and their impact on composite morphology. Microscopic analysis (Figure 3) revealed that WPCs made with larger particles (P20R40) contained significantly larger and more numerous microvoids compared with WPCs with smaller particles. These larger particles are more difficult to fully encapsulate within the molten polymer during compounding, leading to poor filler-matrix adhesion and the formation of voids at the interface. These voids act as physical pathways for water to penetrate and accumulate within the composite structure (Clemons 2002, Wang and Morell 2004, Izekor *et al.* 2013).

Microscopic examination of these samples confirmed a more uniform dispersion of the smaller particles within the LDPE matrix and a notable reduction in microvoid size and quantity. This improved encapsulation effectively seals the hydrophilic surfaces and creates a less continuous pathway for moisture penetration, thus enhancing the composite's water resistance (Wang and Morrell 2004, Xu *et al*. 2021). The better dimensional stability (lower *TS*) of these samples is due to reduced water absorption.

The trends observed for both *WA* and *TS* are fundamentally linked, as the physical swelling of the composite is a direct result of water absorption by the wood filler. These findings are

consistent with extensive research, which has shown that finer wood particles lead to better water resistance and dimensional stability in WPCs due to improved filler dispersion and reduced void content (Takatani *et al*. 2000, Wang and Morrell 2004, Izekor *et al*. 2013, Gozdecki and Wilczyński 2015, Xu *et al*. 2021).

Table 3: Summary of the effect of treatment on the physical properties of falcata WPC

Treatments (Mesh code - SD: LDPE)	Moisture Content, % ± SE	Relative Density ± SE	Water Absorption (WA), % ± SE		Thickness Swelling (TS), % ± SE	
			2 h	24 h	2 h	24 h
Control - 0:100	0,00 ± 0,00 c	0,95 ± 0,01 d	0,71 ± 0,08 bc	1,18 ± 0,16 c	0,037 ± 0,02 d	0,045 ± 0,01 d
P20R40 - 30:70	0,82 ± 0,03 b	1,02 ± 0,01 c	1,63 ± 0,15 a	1,82 ± 0,18 a	0,204 ± 0,02 a	0,337 ± 0,05 a
P40R60 - 30:70	0,72 ± 0,18 b	1,03 ± 0,00 bc	0,92 ± 0,07 b	1,28 ± 0,09 bc	0,097 ± 0,02 bc	0,189 ± 0,04 bc
P60 - 30:70	0,80 ± 0,08 b	1,04 ± 0,00 b	0,65 ± 0,11 bc	0,95 ± 0,09 c	0,068 ± 0,03 cd	0,136 ± 0,05 cd
P40R60 - 40:60	1,30 ± 0,13 a	1,05 ± 0,01 b	0,81 ± 0,04 b	1,64 ± 0,11 ab	0,132 ± 0,01 b	0,297 ± 0,03 ab
P60 - 40:60	1,03 ± 0,14 ab	1,09 ± 0,00 a	0,47 ± 0,10 c	1,11 ± 0,15 c	0,067 ± 0,01 cd	0,192 ± 0,04 cd

± SE is standard error

For each property, means with same letter are not significantly different at α=0,05 using DMRT

Table 4: Summary of the effect of treatment on the mechanical properties of falcata WPC

Treatments (Mesh code - SD: LDPE)	Tensile Properties			Flexural Properties			Izod Impact Energy ($J.m^{-1}$) ± SE
	Strength, (MPa) ± SE	Modulus, (GPa) ± SE	Elongation, (%) ± SE	Strength, (MPa) ± SE	Modulus, (GPa) ± SE	Deflection, (%) ± SE	
Control - 0:100	7,32 ± 0,11 d	0,49 ± 0,02 c	2,50 ± 0,00 a	16,97 ± 0,56 c	0,59 ± 0,01 d	4,89 ± 0,12 a	168,09 ± 18,02 a
P20R40 - 30:70	9,11 ± 0,33 b	0,84 ± 0,03 b	2,26 ± 0,09 b	21,22 ± 0,16 b	1,14 ± 0,05 c	4,02 ± 0,19 b	81,32 ± 15,48 b
P40R60 - 30:70	9,64 ± 0,15 b	0,82 ± 0,01 b	2,43 ± 0,07 ab	21,09 ± 0,12 b	1,25 ± 0,02 c	3,51 ± 0,08 c	55,97 ± 3,30 bc
P60 - 30:70	10,45 ± 0,27 a	0,86 ± 0,02 b	2,32 ± 0,09 ab	24,27 ± 0,27 a	1,37 ± 0,03 b	3,60 ± 0,16 c	55,37 ± 9,18 bc
P40R60 - 40:60	8,27 ± 0,23 c	0,98 ± 0,03 a	1,45 ± 0,05 c	20,91 ± 0,64 b	1,64 ± 0,06 a	2,26 ± 0,10 d	42,67 ± 4,27 c
P60 - 40:60	9,01 ± 0,14 b	0,96 ± 0,03 a	1,51 ± 0,02 c	21,02 ± 0,41 b	1,61 ± 0,02 a	2,29 ± 0,04 d	43,54 ± 6,22 c

± SE is standard error

For each property, means with same letter are not significantly different at α=0,05 using DMRT.

Mechanical properties of WPC

The mechanical properties of the WPCs were evaluated through tensile, flexural, and Izod impact tests. Statistical analysis using ANOVA confirmed significant differences in all measured properties (all $p<0,0001$) across the various sample formulations.

Tensile properties

The LDPE control (0:100) exhibited a tensile strength ($T\sigma$) of 7,32 MPa and a tensile modulus (T_E) of 0,49 GPa (Table 4). The inclusion of sawdust significantly enhanced both properties, with the maximum $T\sigma$ reaching 10,45 MPa for P60 (30:70 ratio), representing a 43 % increase over the LDPE control. Regarding the stiffness and ductility, the T_E was primarily governed by filler concentration, with the higher 40:60 ratio composites exhibiting T_E values up to 0.98 GPA, which is a 100% increase over the control. Conversely, the tensile strain ($T\epsilon$) was inversely proportional to sawdust content, with the lowest $T\epsilon$ (1,45 %) found in the 40:60 ratio, a value considerably lower than the LDPE control (2,50%).

The maximum value of $T\sigma$ is quantitatively consistent with the typical range for non-compatibilized LDPE/wood flour composites, which often fall between 6 MPa and 12 MPa for similar filler loadings. For comparison, Gulitah and Liew (2018) reported a $T\sigma$ of 5,55 MPa for a 30 % wood fiber/LDPE composite, while Wolcott and Englund (1999) disclosed 11,2 MPa. Studies using much lower fiber proportions, such as 15 wt.%, have reported even higher strengths, reaching 12,64 MPa (Gomes *et al.* 2023).

These results confirm the effective reinforcing role of the sawdust relative to the specific LDPE grade used. The finding that finer sawdust particles (P60) yield higher $T\sigma$ is substantiated by the principle that smaller particles facilitate better dispersion, creating a larger effective surface area for optimized stress transfer at the polymer-fiber interface (Stark and Rowlands 2003). While the T_E increased significantly, the gain remains at the lower end of the WPC spectrum. This comparatively lower T_E suggests that the lack of a coupling agent results in an inefficient load transfer across the interface, thereby limiting the ultimate stiffening effect provided by the wood fibers. For instance, chemically coupled WPCs are known to improve modulus by up to 30 % more than the uncoupled systems (Yuan *et al.* 2008). Furthermore, the reduction in $T\epsilon$ is attributed to the rigid wood particles acting as stress concentrators that disrupt the matrix continuity, which inhibits the plastic deformation of the polymer (Stark and Rowlands 2003, Rahman *et al.* 2018).

Flexural properties

The flexural strength ($F\sigma$) and flexural modulus (F_E) of the WPCs demonstrated a more pronounced reinforcement than the tensile properties. Specifically, the WPCs showed a 23 % to 43 % increase in $F\sigma$ and a 93 % to 178 % increase in F_E over the LDPE control (16,97 MPa and 0,59 GPa, respectively). The maximum values obtained were $F\sigma$ = 24,27 MPa and F_E=1,64 GPa. To contextualize these findings and evaluate their performance against broader industry benchmarks, Table 5 presents a comparison of the current results against WPCs utilizing other common thermoplastics matrices, such as HDPE and PP.

Comparative analysis of Table 5 reveals that the $F\sigma$ of the LDPE-falcata WPCs (up to 24,27 MPa) falls within the typical range reported for many HDPE-based composites (≈ 21–31 MPa), aligning well with results for recycled HDPE and HDPE-WF800 (Chaharmahali *et al.* 2010, Chaudemanche *et al.* 2018). However, the F_E (maximum 1,64 GPa) is noticeably below the typical 2,5–3,8 GPa range observed for HDPE and PP WPCs. For example, PP-based WPCs typically exhibit 28 % to 76 % higher flexural stiffness than the material produced in this study (Stark and Rowlands 2003).

The overall lower stiffness profile compared with HDPE and PP systems is primarily attributed to the inherent material characteristics of the polymer matrix. LDPE possesses a lower degree of crystallinity and a lower intrinsic elastic modulus compared to its high-density or polypropylene counterparts (Posch 2011). While the inclusion of falcata sawdust provides significant reinforcement to the base LDPE, the ultimate stiffness is capped by the flexibility of the recycled matrix itself. Furthermore, variations in particle morphology and the lack of compatibilizers in this specific system may account for the differences in performance relative to the chemically-coupled systems cited in Table 5. Given these properties, the LDPE-falcata WPCs are ideally suited for non-load-bearing applications, such as internal furniture components (e.g., drawer parts, cabinet sidings) or non-structural wall cladding, where moderate strength and high ductility are advantageous.

Table 5: Comparison of the flexural properties of LDPE-falcata WPC against other matrices of WPCs that used sawdust (SD) or other lignocellulosic fibers.

Ratio SD:TP:OA	Thermoplastic Matrices	Flexural Properties			Remarks (mesh #, type of sawdust material or WPC product, reference study)
		$F\sigma$ (MPa)	F_E (GPa)	$F\epsilon$ (%)	
30:70	LDPE	24,27	1,37	3,60	P60 SD - This study
40:60	LDPE	21,02	1,61	2,29	P60 SD - This study
35:55:5:5	HDPE-MP-OA	21,3	3.43	-	Decking - WF800 - Chaudemanche *et al.* 2018
40:57:3	PP-MAPP	42,6	3,15	-	Stark and Rowlands 2003
50:50	VPE	~ 22	~ 2,0	-	Najafi *et al.* 2006
50:50	VPP	~ 34	~ 3,8	-	Najafi *et al.* 2006
50:50	RPE	~ 24	~2,5	-	Najafi *et al.* 2006
50:50	RPP	~ 31	` ~3,4	-	Najafi *et al.* 2006
60:40	RHDPE	~ 25	~ 2,7	-	RPB - Chaharmahali *et al.* 2010
70:30	RHDPE	~ 24	~ 2,9	-	RPB - Chaharmahali *et al.* 2010
60:40	RHDPE	~ 31	~ 2,8	-	RMDF - Chaharmahali *et al.* 2010
70:30	RHDPE	~ 28	~ 3,2	-	RMDF - Chaharmahali *et al.* 2010

Ratio is in the order of sawdust (SD), thermoplastic matrix (TP), and other additives (OA) such as compatibilizer, minerals and pigments. Under Remarks, RPB stands for Recycled Particleboard, and RMDF for Recycled Medium Density Fiberboard. The values cited from Najafi *et al.* 2006 and Chaharmahali *et al.* 2010 were approximated from the bar scales of the graphical results.

Izod impact strength

The Izod impact strength (*Iz*) measurements demonstrated the most significant compromise in mechanical properties upon forming the WPCs. The control LDPE showed a high *Iz* of 168,09 $J \cdot m^{-1}$, a value characteristic of a ductile polymer. This was drastically reduced across all falcata WPC samples, with the highest *Iz* recorded at 81,32 $J \cdot m^{-1}$ for the P20R40 (30:70) formulation, representing an approximately 52 % drop compared to the control. Regarding the effects of composition and size, increasing the sawdust content from 30 wt.% to 40 wt.% further decreased *Iz* by 32 % to 46 %. Additionally, a marginal trend was observed where larger

particle sizes (P20R40 at 81,32 J·m⁻¹) slightly enhanced *Iz* compared with smaller particles (P60 at 43,54 J·m⁻¹).

As shown in Table 6, the values obtained in this study (ranging from 43,54 to 81,32 J·m⁻¹) fall within the moderate-to-high end of the typical range reported for uncompatibilized commodity polymer WPCs. For instance, our optimal result is closely comparable to the 79 J·m⁻¹ reported by Stark and Rowlands (2003) for a wood flour-PP WPC at a 40:60 ratio. While Table 6 highlights a broad range of values in the literature—from the very low results of Najafi *et al.* (2006) to the high values of Chaharmahali *et al.* (2010)—the performance of the developed LDPE-falcata system remains robust relative to other uncompatibilized wood/polymer matrices.

This reduction in impact resistance and the observed performance levels relative to other studies are primarily attributed to failure mechanisms and matrix characteristics. The rigid, discontinuous falcata wood particles act as stress concentrators for crack initiation, while the poor interfacial adhesion between the hydrophilic wood and the hydrophobic LDPE matrix suppresses effective energy dissipation mechanisms like matrix shear yielding and crack blunting (de Prá Andrade and Poletto 2021). The inefficient energy transfer from the matrix to the wood leads to premature brittle failure at the weak interface. The fact that our values are on the higher end of the uncompatibilized spectrum, despite the lack of coupling agents, is likely due to the inherent ductility of the recycled LDPE matrix compared to stiffer polymers like PP or HDPE. Furthermore, the differences observed in Table 6 underscore how variations in polymer type, filler morphology, and adherence to testing standards (ASTM D256-10e1 2018) heavily influence energy absorption.

These trends are highly consistent with composite theory and earlier findings by Chaharmahali *et al.* (2010). The impact energy absorption scales inversely with filler volume fraction because the continuous, ductile polymer matrix—the primary energy-absorbing component—is

progressively diluted while the concentration of crack initiation sites simultaneously rises (Stark and Rowlands 2003, Ramesh *et al.* 2022). The particle size effect is likely related to the crack propagation mechanism. A larger particle requires a greater energy input to either debond or fracture internally (Ashori *et al.* 2011), thus temporarily dissipating more energy. In contrast, a crack can more easily bypass a large number of smaller particles by propagating through the weak interfacial region (Stark and Rowlands 2003, Ramesh *et al.* 2022). Future research should prioritize the use of compatibilizing agents to improve interfacial strength, which remains the most critical factor for mitigating the inherent reduction in *Iz*.

Table 6: Comparison of the impact strength of LDPE-falcata WPC against other matrices of WPCs that used sawdust (SD) or other lignocellulosic fibers.

Ratio	Thermoplastic Matrices	Impact Strength		Remarks (mesh #, type of sawdust material or WPC product, reference study)
		$kJ.m^{-2}$ EN ISO 179	$J.m^{-1}$ (ASTM D256)(2018)	
30:70	LDPE	-	55,37	P60 SD - This study
40:60	LDPE	-	43,54	P60 SD - This study
35:55:5:5	HDPE-MP-OA	3,2 - 4,2	-	Decking - WF800 - Chaudemanche *et al.* 2018
40:57:3	PP-MAPP	-	79	Stark and Rowlands 2003
50:50	VPE	-	~ 5	Najafi *et al.* 2006
50:50	VPP	-	~ 3,8	Najafi *et al.* 2006
50:50	RPE	-	~ 3,9	Najafi *et al.* 2006
50:50	RPP	-	~ 4,1	Najafi *et al.* 2006
60:40	RHDPE	-	~ 420	RPB - Chaharmahali *et al.* 2010
70:30	RHDPE	-	~ 310	RPB - Chaharmahali *et al.* 2010
60:40	RHDPE	-	~520	RMDF - Chaharmahali *et al.* 2010
70:30	RHDPE	-	~ 480	RMDF - Chaharmahali *et al.* 2010

Ratio is in the order of sawdust (SD), thermoplastic matrix (TP), and other additives (OA) such as compatibilizer, minerals and pigments. Under Remarks, RPB stands for Recycled Particleboard, and RMDF for Recycled Medium Density Fiberboard. The values cited from Najafi *et al.* 2006 and Chaharmahali *et al.* 2010 were approximated from the bar scales of the graphical results.

Conclusions

This investigation confirms the technical viability of utilizing falcata sawdust and recycled LDPE as sustainable raw materials for WPCs in the Philippines. The resulting composites demonstrate comparable dimensional stability and significantly higher mechanical stiffness compared to the neat polymer matrix, addressing a critical requirement for functional furniture and construction components.

The study reveals that the mechanical performance of these composites is fundamentally governed by the interplay between particle size and filler loading. Finer sawdust particles (P60) at a 30 % loading ratio represent the optimal configuration for maximizing tensile and flexural strength and stiffness. This is attributed to the increased effective surface area of smaller particles, which promotes more uniform dispersion and facilitates better stress transfer across the polymer-fiber interface.

However, the results underscore a significant performance trade-off regarding energy absorption. While the finer particles favor stiffness, they simultaneously increase the concentration of stress-initiation sites, leading to a marked reduction in impact resistance. Conversely, the P20R40 formulation at a 30 % ratio was identified as superior for impact toughness. This suggests that larger particle distributions may be more effective at dissipating energy through crack-blunting mechanisms or internal fiber fracture, making them more suitable for applications where toughness and a "wood-like" aesthetic are prioritized over absolute stiffness.

The findings demonstrate that the properties of falcata-LDPE WPCs can be tailored based on particle size selection to meet specific industrial requirements. To move from this preliminary investigation toward full-scale industrial adoption, future research should focus on the integration of chemical compatibilizers. Such additives are essential to bridge the interfacial

gap between the hydrophilic wood filler and the hydrophobic matrix, potentially mitigating the current trade-off between stiffness and impact resistance and further elevating the material's structural performance.

Authorship contributions

J. P. J. J.: Conceptualization, data curation, formal analysis, investigation, methodology, resources, supervision, validation, visualization, writing: review, editing of original and final draft, revision and finalization of the manuscript.

Acknowledgments

The author gratefully acknowledges the funding support provided by DOST-FPRDI (project code FPRD 20150009) and partly from a PCAARRD funded-project on young falcata trees for the completion of this work. Sincere thanks are extended to the project support staff for their invaluable assistance and to Ms. Emerita Barile for the language editing. Special appreciation goes to Engr. Josephine P. Carandang for spearheading the initial studies that laid the foundation for this research. The author also expresses deep gratitude to DOST-ITDI for facilitating the production and mechanical testing, with special thanks to Dr. Marissa A. Paglicawan for her guidance and for granting access to ITDI's production facilities.

References:

Alipon, M.A.; Bondad, E.O.; Gilbero, D.M. Jimenez, J.J.P.; Domingo, E.P.; Marasigan, O.S. 2021. Anatomical Properties and Utilization of 3-, 5-, and 7-yr-old Falcata (Falcataria moluccana (Miq.)) Barneby & JW Grimes) from Caraga Region, Mindanao Philippines. *Philippine Journal of Science* 150(5): 1307-1319. http://dx.doi.org/10.56899/150.05.38

ASTM International. ASTM 2018. Methods for Determining the Izod Pendulum Impact Resistance of Plastics ASTM D256-10e1. 2018. ASTM International. West Conshohocken, USA.

ASTM International. ASTM 2017. Method for Tensile Properties of Plastics. ASTM D638-02a. 2017. ASTM International. West Conshohocken, USA.
ASTM International. ASTM. 2017. Methods for Evaluating Properties of Wood-Base Fiber and Particle Panel Materials. ASTM D1037-99. 2017. ASTM International. West Conshohocken, USA.
ASTM International. ASTM. 2017. Methods for Flexural Properties of Unreinforced and Reinforced Plastics and Electrical Insulating Materials. ASTM D790-15e2. 2017. ASTM International. West Conshohocken, USA.
ASTM International. ASTM. 2019. Guide for Evaluating Mechanical and Physical Properties of Wood-Plastic Composite Products. ASTM D7031-11. 2019. ASTM International. West Conshohocken, USA.
ASTM International. ASTM. 2022. Methods for Density and Specific Gravity (Relative Density) of Wood and Wood-Based Materials. ASTM D2395-17. 2022. ASTM International. West Conshohocken, USA.
Antwi-Boasiako, C.; Ansah, A.O.O.; Glalah, M. 2022. Physico-mechanical properties of wood–plastic composites from *Triplochiton scleroxylon* K. Schum wood-residue and post-consumer polyethylene waste as construction materials. *International Wood Products Journal* 13(1): 50-56. https://doi.org/10.1080/20426445.2021.2014026
Ashori, A.; Kiani, H.; Mozaffari, S.A. 2011. Mechanical properties of reinforced polyvinyl chloride composites: Effect of filler form and content. *Journal of Applied Polymer Science* 120(3): 1788-1793. https://doi.org/10.1002/app.33378
Aumnate, C.; Gamonpilas, C.; Kruenate, J. 2010. Effect of ethylene vinyl acetate on the rheological and mechanical behavior of low-density polyethylene-based greenhouse film. *Advanced Materials Research*. 93: 475-478.
https://doi.org/10.4028/www.scientific.net/AMR.93-94.475
Bello, R.S. 2017. Characterization of sawdust produced from circular, chain and band sawing machines. *Bioprocess Engineering* 1(1): 21-29.
https://www.sciencepublishinggroup.com/article/10.11648/j.be.20170101.14
Berger, M.J.; Stark, N.M. 1997. Investigations of species effects in an injection-molding-grade, wood-filled polypropylene. In Proceedings of the fourth international conference on wood fiber-plastic composites, Madison, WI. USA. 12 -14 May 1997, pp. 19-25.
https://docslib.org/doc/11746649/investigations-of-species-effects-in-an-injection-molding-grade-wood-filled-polypropylene
Berzin, F.; Vergnes, B. 2021. Thermoplastic natural fiber-based composites. In: *Fiber reinforced composites.* Woodhead Publishing, Elsevier, Amsterdam, Netherlands,. pp. 113-139 https://doi.org/10.1016/B978-0-12-821090-1.00015-6. ISBN: 978-0-12-821090-1
Bledzki, A.K.; Gassan, J. 1999. Composites reinforced with cellulose-based fibres. *Prog Polym Sci* 24(2): 221-274. https://doi.org/10.1016/S0079-6700(98)00018-5
Caulfield, D.F.; Clemons, C.; Jacobson, R.E.; Rowell, R.M. 2005. Wood/Nonwood Thermoplastic Composites. In: *Handbook of wood chemistry and wood composites*. CRC Press, Boca Raton, Florida, USA, pp. 366-378. https://doi.org/10.1201/b12487. ISBN 0-8493-1588-3.
Chaharmahali, M.; Mirbagheri, J.; Tajvidi, M.; Najafi, S. K.; Mirbagheri, Y. 2010. Mechanical and physical properties of wood-plastic composite panels. *Journal of Reinforced Plastics and Composites.* 29(2): 310-319. https://doi.org/10.1177/0731684408093877
Chaharmahali, M.; Tajvidi, M.; Najafi, S. K. 2008. Mechanical properties of wood plastic composite panels made from waste fiberboard and particleboard. *Polymer composites*. 29(6): 606-610. https://doi.org/10.1002/pc.20434
Chaudemanche, S.; Perrot, A.; Pimbert, S.; Lecompte, T.; Faure, F. 2018. Properties of an industrial extruded HDPE-WPC: The effect of the size distribution of wood flour particles.

Construction and Building Materials. 162: 543-552. https://doi.org/10.1016/j.conbuildmat.2017.12.061
Clemons, C. 2002. Wood-plastic Composites in the United States: The interfacing of two Industries. *Forest Products Journal* 52(6): 10-18. https://research.fs.usda.gov/treesearch/8778
Clemons, C. 2010. Wood flour. In: *Functional Fillers for Plastics*: Second, updated and enlarged edition. John Wiley & Sons. pp. 269 - 290. ISBN: 978-3-527-32361-5.
de Prá Andrade, M.; Poletto, M. 2021. Wood treatments and interfacial bonding in wood-plastic composites. In: *Wood Polymer Composites: Recent Advancements and Applications*. Springer, Singapore, pp. 43-65. https://doi.org/10.1007/978-981-16-1606-8_3. ISBN978-981-16-1605-1
Delviawan, A.; Kojima, Y.; Kobori, H.; Suzuki, S.; Aoki, K.; Ogoe, S. 2019. The effect of wood particle size distribution on the mechanical properties of wood-plastic composite. *Journal of Wood Science* 65(1). e67. https://doi.org/10.1186/s10086-019-1846-9
Eduagin, R.T.; Galarrita, R.J.L.; Calixtro, J.F.; Oclaman, F.D.; Namoco, C.S. 2021. Utilization of falcata sawdust briquettes as an alternative solid fuel. *Journal of Engineering and Applied Sciences* 16(8): 880-884. https://hal.science/hal-04172864/
Espert, A.; Vilaplana, F.; Karlsson, S. 2004. Comparison of water absorption in natural cellulosic fibres from wood and one-year crops in polypropylene composites and its influence on their mechanical properties. *Composites Part A: Applied science and manufacturing*. 35(11), 1267-1276. https://doi.org/10.1016/j.compositesa.2004.04.004
Faker, M.; Aghjeh, M. R.; Ghaffari, M.; Seyyedi, S.A. 2008. Rheology, morphology and mechanical properties of polyethylene/ethylene vinyl acetate copolymer (PE/EVA) blends. *European Polymer Journal.* 44(6): 1834-1842. https://doi.org/10.1016/j.eurpolymj.2008.04.002
Flores-Hernandez, M. A.; González, I. R.; Lomeli-Ramirez, M. G.; Fuentes-Talavera, F. J.; Silva-Guzman, J. A.; Cerpa-Gallegos, M. A.; García-Enriquez, S. 2014. Physical and mechanical properties of wood plastic composites polystyrene-white oak wood flour. *Journal of composite materials* 48(2): 209-217. https://doi.org/10.1177/0021998312470149
Forest Management Bureau - Department of Environment and Natural Resources. 2023. *Philippine Forestry Statistics*. Quezon City, Philippines.
Gacitúa, W.; Wolcott, M. 2009. Morphology of wood species affecting wood-thermoplastic interaction: Microstructure and mechanical adhesion. *Maderas. Ciencia y Tecnología* 11(3): 217-231. http://dx.doi.org/10.4067/S0718-221X2009000300005
Gomes, D. A. C.; de Novais Miranda, E. H.; de Araújo Veloso, M. C. R.; da Silva, M. G.; Ferreira, G. C.; Mendes, L. M.; Júnior, J. B. G. 2023. Production and characterization of recycled low-density polyethylene/amazon palm fiber composites. *Industrial Crops and Product* 201. e116833. https://doi.org/10.1016/j.indcrop.2023.116833
Gozdecki, C; Wilczyński, A. 2015. Effects of wood particle size and test specimen size on mechanical and water resistance properties of injected wood-high density polyethylene composites. *Wood and Fiber Science* 47(4): 1-10. https://wfs.swst.org/index.php/wfs/article/view/2366/2254
Granada, J.B.R.; Anggut, A.O.; Tama, F.S.I.; Abarca, R.R.; Ogdiman, R.A.; Pahunang, R.R. 2024. Response surface methodology optimization of sodium diclofenac adsorption using activated carbon derived from falcata tree sawdust. *Industrial Crops and Products* 221. e119272. https://doi.org/10.1016/j.indcrop.2024.119272
Gulitah, V.; Liew, K. C. 2018. Effect of plastic content ratio on the mechanical properties of wood-plastic composite (WPC) made from three different recycled plastic and acacia fibres. *Transactions on Science and Technology*. 5(2): 184-189. https://tost.unise.org/pdfs/vol5/no2/5x2x184x189.html

Hu, X.; Li, D.; Li, L. 2020. Weathering characteristics of wood-plastic composites compatibilized with ethylene vinyl acetate. *BioResources* 15(2): 3930-3944. http://dx.doi.org/10.15376/biores.15.2.3930-3944
Israel, D.C.; Bunao, D.F.M. 2017. Value chain analysis of the wood processing industry in the Philippines, PIDS Discussion Paper Series, No. 2017-05, Philippine Institute for Development Studies (PIDS), Quezon City. https://hdl.handle.net/10419/173582
Izekor, D.N.; Amiandamhen, S.O.; Agbarhoaga, O.S. 2013. Effects of geometric particle sizes of wood flour on strength and dimensional properties of wood plastic composites. *Journal of Applied and Natural Science* 5(1): 194-199. http://dx.doi.org/10.31018/jans.v5i1.305
Jimenez J.J.P.; Escobin, R.P.; Conda, J.M. 2015. Profile of wood species used in local and imported plywood and their bond performance. *Philippine Forest Products Journal* 6(1): 43-58.
Jimenez J.J.P.; Gilbero, D.M.; Alipon, M.A. 2021. Veneer and plywood properties of yemane (*Gmelina arborea* Roxb.) from 3-, 5-, and 7-year-old plantation trees. *International Wood Products Journal* 12(4): 277-286. https://doi.org/10.1080/20426445.2021.1979823
Jimenez J.J.P.; Gilbero, D.M.; Alipon, M.A. 2022. Evaluation of Young Falcata Plus-Trees for Veneer and Plywood Production in the Philippines. *Philippine Journal of Science* 151(6A): 2081-2092. https://doi.org/10.56899/151.6A.02
Jimenez, J.J.P.; Mari, E.L.; Villena, E.M.; Cabangon, R.J. 2013. Utilization of spent tea leaves and waste plastics for composite boards. *Philippine Forest Products Journal* 4(1): 29-36.
Kamdem, D.P.; Jiang, H.; Cui, W.; Freed, J.; Matuana, L.M. 2004. Properties of wood plastic composites made of recycled HDPE and wood flour from CCA-treated wood removed from service. *Composites Part A: Applied Science and Manufacturing* 35(3): 347-355. https://doi.org/10.1016/j.compositesa.2003.09.013
Kellogg, R. M.; Wangaard, F. F. 1969. Variation in the cell-wall density of wood. *Wood and Fiber Science* 3: 180-204. https://wfs.swst.org/index.php/wfs/article/view/1352
Khonsari, A.; Taghiyari, H.R.; Karimi, A.; Tajvidi, M. 2015. Study on the effects of wood flour geometry on physical and mechanical properties of wood-plastic composites. *Maderas Ciencia y Tecnología* 17(3): 545-558. http://dx.doi.org/10.4067/S0718-221X2015005000049
Kormin, S.; Kormin, F.; Beg, M.D.H. 2019. Study on the biodegradability and water adsorption of ldpe/sago starch blend. *Journal of Physics: Conference Series* 1150 (1). 012033. https://iopscience.iop.org/article/10.1088/1742-6596/1150/1/012033/meta
Maharani, R.; Yutaka, T.; Yajima, T.; Minoru, T. 2010. Scrutiny on physical properties of sawdust from tropical commercial wood species: Effects of Different Mills and Sawdust's Particle Size. *Indonesian Journal of Forestry Research* 7(1): 20-32. https://doi.org/10.20886/ijfr.2010.7.1.20-32
Mračková, E.; Krišťák, Ľ.; Kučerka, M.; Gaff, M.; Gajtanska, M. 2016. Creation of wood dust during wood processing: Size analysis, dust separation, and occupational health. *BioResources* 11(1): 209-222. https://doi.org/10.15376/biores.11.1.209-222
Najafi, S. K.; Hamidinia, E.; Tajvidi, M. 2006. Mechanical properties of composites from sawdust and recycled plastics. *Journal of Applied Polymer Science* 100(5): 3641-3645. https://doi.org/10.1002/app.23159
Najafi, S. K.; Sharifnia, H.; Tajvidi, M. 2008. Effects of water absorption on creep behavior of wood-plastic composites. *Journal of Composite Materials* 42(10): 993-1002. https://doi.org/10.1177/0021998307088608
Paglicawan, M.; Emolaga, C.S.; Jimenez, J.J.P. 2025. Properties of Tobacco Stalks as Reinforcement in Natural Fiber Composites. *Philippine Journal of Science* 154(4): 967-982. https://doi.org/10.56899/154.04.16.

Paglicawan, M.; Emolaga, C.S.; Jimenez, J.J.P.; Monsada, A.M.; Marasigan, D.D.; Villanueva, N.M.; Co, J.F. 2022. Thermoplastic composite material comprising wood byproducts. PH/ Utility Model Registration No.: 2/2022/050073.
Pham, N.T.H. 2021. Characterization of low-density polyethylene and LDPE-based/ethylene-vinyl acetate with medium content of vinyl acetate. *Polymers* 13(14). e2352. https://doi.org/10.3390/polym13142352
Posch, W. 2011. Polyolefins. In: *Applied Plastics Engineering Handbook*. William Andrew Publishing. Elsevier, Amsterdam, Netherlands, pp 23-48. https://www.sciencedirect.com/book/9781437735147/applied-plastics-engineering-handbook ISBN: 978-1-4377-3514-7
Pożoga, M.I.; Szczepanek, M. 2021. Analysis of Particles' Size and Degree of Distribution of a Wooden Filler in Wood-Polymer Composites. *Materials* 14(21). e6251. https://doi.org/10.3390/ma14216251
Radoor, S.; Karayil, J.; Shivanna, J.M.; Siengchin, S. 2021. Water Absorption and Swelling Behaviour of Wood Plastic Composites. In: *Wood Polym Compos.* Springer, Singapore. pp 195–212. http://dx.doi.org/10.1007/978-981-16-1606-8_10. ISBN978-981-16-1605-1
Rahman, K.S.; Islam, M.N.; Rahman, M.M.; Hannan, M.O.; Dungani, R.; Khalil, H.A. 2013. Flat-pressed wood plastic composites from sawdust and recycled polyethylene terephthalate (PET): physical and mechanical properties. *SpringerPlus* 2. e629. https://doi.org/10.1186/2193-1801-2-629
Rahman, K.S.; Islam, M.N.; Ratul, S.B.; Dana, N.H.; Musa, S.M.; Hannan, M.O. 2018. Properties of flat-pressed wood plastic composites as a function of particle size and mixing ratio. *Journal of Wood Science* 64: 279-286. https://doi.org/10.1007/s10086-018-1702-3
Ramesh, M.; Rajeshkumar, L. N.; Srinivasan, N.; Kumar, D.V.; Balaji, D. 2022. Influence of filler material on properties of fiber-reinforced polymer composites: A review. *e-Polymers* 22(1): 898-916. https://doi.org/10.1515/epoly-2022-0080
Ramli, R. A. 2024. A comprehensive review on utilization of waste materials in wood plastic composite. *Materials Today Sustainability* 27. e100889. https://doi.org/10.1016/j.mtsust.2024.100889
Samyn, P. 2024. Challenges for Wood–Plastic Composites: Increasing Wood Content and Internal Compatibility. *Environmental and Earth Sciences Proceedings* 31(1): e1. https://doi.org/10.3390/eesp2024031001
Sandquist, D.; Thumm, A.; Dickson, A.R. 2020. The influence of fines material on the mechanical performance of wood fiber polypropylene composites. *BioResources* 15(1): 457-468. https://doi.org/10.15376/biores.15.1.457-468
Smith, P.M.; Wolcott, M.P. 2006. Opportunities for wood/natural fiber-plastic composites in residential and industrial applications. *Forest Products Journal* 56(3): 4-11. http://kb.forestprod.org/Main/ind/?id=67931
Spear, M.J.; Eder, A.; Carus, M. 2015. Wood polymer composites. In: *Wood Composites.* Woodhead Publishing. Elsevier, Amsterdam, Netherlands, pp. 195-249. https://doi.org/10.1016/B978-1-78242-454-3.00010-X. ISBN: 978-1-78242-454-3
Stark, N.M.; Rowlands, R.E. 2003. Effects of wood fiber characteristics on mechanical properties of wood/polypropylene composites. *Wood Fiber Sci* 35(2): 167-174. https://wfs.swst.org/index.php/wfs/article/view/590
Sun, C. C. 2005. True density of microcrystalline cellulose. *Journal of pharmaceutical sciences* 94(10): 2132-2134. https://doi.org/10.1002/jps.20459
Tajvidi, M.; Najafi, S. K.; Moteei, N. 2006. Long-term water uptake behavior of natural fiber/polypropylene composites. *Journal of Applied Polymer Science* 99(5): 2199-2203. https://doi.org/10.1002/app.21892

Takatani, M.; Ito, H.; Ohsugi, S.; Kitayama, T.; Saegusa, M.; Kawai, S.; Okamoto, T. 2000. Effect of lignocellulosic materials on the properties of thermoplastic polymer/wood composites. *Holzforschung* 54(2):197-200. https://doi.org/10.1515/HF.2000.033
Vítěz, T.; Trávníček, P. 2010. Particle size distribution of sawdust and wood shavings mixtures. *Research in Agricultural Engineering* 56(4):154-158. https://rae.agriculturejournals.cz/pdfs/rae/2010/04/05.pdf
Wang, W.; Morell. J.J. 2004. Water sorption characteristics of two wood-plastic composites. *Forest Products Journal* 54 (12): 209-212. http://hdl.handle.net/1957/26271
Wolcott, M.P.; Englund, K. 1999. A technology review of wood–plastic composites. In Proceedings of the 33rd International Particleboard and Composite Materials Symposium. Pullman WA. 13-15 April 1999. pp. 103-111.
World Bank Group. 2021. Market Study for the Philippines: Plastics Circularity Opportunities and Barriers. Marine Plastics Series, East Asia and Pacific Region. Washington DC., USA. https://doi.org/10.1596/35295
Xu, K.; Du, G.; Wang, S. 2021. Wood plastic composites: their properties and applications. In: *Engineered Wood Products for Construction*. IntechOpen. 92960, pp. 197-221. https://doi.org/10.5772/intechopen.98918. ISBN: 978-1-83962-771-2.
Yuan, Q.; Wu, D.; Gotama, J.; Bateman, S. 2008. Wood fiber reinforced polyethylene and polypropylene composites with high modulus and impact strength. *Journal of Thermoplastic Composite Materials* 21(3): 195-208. https://doi.org/10.1177/0892705708089472
Zepeda-Cepeda, C.O.; Goche-Télles, J.R.; Palacios-Mendoza, C.; Moreno-Anguiano, O.; Núñez-Retana, V.D.; Heya, M.N.; Carrillo-Parra, A. 2021. Effect of sawdust particle size on physical, mechanical, and energetic properties of *Pinus durangensis* briquettes. *Applied sciences* 11(9). e3805. https://doi.org/10.3390/app11093805
Zimmermann, M.V.; Turella, T.C.; Santana, R.M.; Zattera, A.J. 2014. The influence of wood flour particle size and content on the rheological, physical, mechanical and morphological properties of EVA/wood cellular composites. *Materials & Design* 57: 660-666. http://dx.doi.org/10.1016/j.matdes.2014.01.010